DRAFT VERSION JUNE 29, 2010
Preprint typeset using LaTeX style emulateapj v. 03/07/07

THE *KEPLER* LIGHT CURVE OF V344 LYR: CONSTRAINING THE THERMAL-VISCOUS LIMIT CYCLE INSTABILITY

J. K. CANNIZZO[1,2], M. D. STILL[3,4], S. B. HOWELL[5], M. A. WOOD[6], AND A. P. SMALE[2]

Draft version June 29, 2010

ABSTRACT

We present time dependent modeling based on the accretion disk limit cycle model for a 90 d light curve of the short period SU UMa-type dwarf nova V344 Lyr taken by *Kepler*. The unprecedented precision and cadence (1 minute) far surpass that generally available for long term light curves. The data encompass a superoutburst, preceded by three normal (i.e., short) outbursts and followed by two normal outbursts. The main decay of the superoutburst is nearly perfectly exponential, decaying at a rate $\sim$12 d mag^{-1}, while the much more rapid decays of the normal outbursts exhibit a faster-than-exponential shape. We show that the standard limit cycle model can account for the light curve, without the need for either the thermal-tidal instability or enhanced mass transfer.

Subject headings: accretion, accretion disks - binaries: close - cataclysmic variables - stars: dwarf novae

1. INTRODUCTION

Dwarf novae constitute a subclass of the cataclysmic variables, semi-detached interacting binaries in which a Roche-lobe filling secondary transfers matter to a more massive, and also more compact primary. The transferred material possesses angular momentum, and therefore can only "fall" toward the primary down to a radius determined by its specific angular momentum (Lubow & Shu 1975). This angular momentum barrier is overcome by angular momentum transport within the accretion disk which carries angular momentum outward and mass inward. Current thinking about the physical mechanism responsible for accretion centers on the magneto-rotational instability (=MRI; Balbus & Hawley 1998) in which the shearing amplification of a weak seed magnetic field leads to turbulent transport.

V344 Lyr is a short period dwarf nova, of subtype SU UMa ($P_{\rm orb}$ = 2.06 h; Still et al. 2010) exhibiting a supercycle pattern (109.6 d; Kato et al. 2002) consisting of superoutbursts separated by normal outbursts. Superoutbursts are long outbursts with slow, exponential decays exhibiting superhumps – modulations in the light curve at a period greater than the orbital period by a few percent. The data presented in Kato et al. reveal only the brightest portions of the superoutbursts; the fainter portions and all of the normal outbursts lie below the lower limit of detection.

The *Kepler* data set for V344 Lyr (*Kepler* ID 7659570) – 90 d at 1 min cadence – provides an extraordinary resource for accretion disk modelers. The accretion disk limit cycle mechanism, which is currently employed to account for dwarf nova outbursts, is based on the storage of material during quiescence in a non-steady-state configuration, followed by a dumping of matter onto the accreting WD when a critical surface density is attained in the disk, producing an outburst. During outburst the disk is roughly in steady state, except for the action of a cooling front that begins at the outer disk and moves inward. The thermal-viscous limit cycle model is not a complete model for the accretion disk, but rather primarily a model for the outbursts; for instance it fails to account for the high X-ray luminosities and column densities seen in dwarf novae in quiescence (Mukai, Zietsman, & Still 2009).

Previous attempts at constraining physical parameters of the model have relied on AAVSO (American Association of Variable Star Observers) and RASNZ (Royal Astronomical Society of New Zealand) data for the long term light curves. These data are typically given as 1d means, with large attendant error bars ($\sim$0.3–0.5 mag). The *Kepler* data provide an entirely new level of precision, and allow detailed model constraints. The viscosity parameter α (Shakura & Sunyaev 1973) sets the disk time scales. To first order, $\alpha_{\rm cold}$ controls the recurrence time for outbursts, and $\alpha_{\rm hot}$ sets the duration of the outbursts. Previous efforts, for instance by Smak (1984=S84), utilized the "Bailey relation" relating the rate of the fast decay in DNe with orbital period to infer that $\alpha_{\rm hot} \simeq 0.1 - 0.2$. This remains the only firm constraint we have in astronomy for α in ionized gas, and has served as a benchmark value for modelers calculating the efficiency of the MRI in accretion disks (e.g., Hirose et al 2009).

Our goal in this work is to find model parameters that can account for the gross properties of the long term V344 Lyr light curve. There will be additional features in the light curve that can be compared to the detailed model light curves in order to gain insight into shortcomings of the model. We also investigate systematic effects such as the number of grid points and time step size.

In section 2 we present an overview of the physics of accretion disks. Section 3 discusses the V344 Lyr light curve, section 4 presents a review of viscous decays in several well-studied dwarf novae, section 5 details the numerical model, section 6 presents the results, section 7 contains a discussion, and section 8 sums up.

2. ACCRETION DISK PHYSICS

In the accretion disk limit cycle model, gas accumulates in quiescence and accretes onto the central object in outburst (e.g., Cannizzo 1993a, Lasota 2001 for reviews). The phases of quiescence and outburst are mediated by the action

[1] CRESST/Joint Center for Astrophysics, University of Maryland, Baltimore County, Baltimore, MD 21250, John.K.Cannizzo@nasa.gov
[2] Astroparticle Physics Laboratory, NASA-Goddard Space Flight Center, Greenbelt, MD 20771
[3] Bay Area Environmental Research Inst., Inc., 560 Third St. W, Sonoma, CA 95476, Martin.D.Still@nasa.gov
[4] NASA-Ames Research Center, Moffet Field, CA 94035
[5] National Optical Astronomy Observatory, Tucson, AZ 85719
[6] Department of Physics and Space Sciences, Florida Institute of Technology, 150 W. University Blvd., Melbourne, FL 32901

of heating and cooling fronts that transverse the disk and bring about phase transitions between low and high states, consisting of neutral and ionized gas, respectively. During quiescence, when the surface density $\Sigma(r)$ at some radius within the disk exceeds a critical value $\Sigma_{\rm max}(r)$, a transition to the high state is initiated; during outburst, when $\Sigma(r)$ drops below a different critical value $\Sigma_{\rm min}(r)$, a transition to the low state is initiated. Low-to-high transitions can begin at any radius, whereas high-to-low transitions begin at the outer disk edge. This situation comes about because in the outburst disk $\Sigma(r) \propto r^{-3/4}$ (roughly), and the critical surface densities both increase with radius. Since the disk mass accumulated in quiescence is bounded by $\Sigma_{\rm max}(r)$ and $\Sigma_{\rm min}(r)$, one can define a maximum disk mass

$$M_{\rm disk,\ max} = \int 2\pi r dr \Sigma_{\rm max}(r) \quad (1)$$

and a minimum disk mass

$$M_{\rm disk,\ min} = \int 2\pi r dr \Sigma_{\rm min}(r) \quad (2)$$

which will bound the general, time dependent disk mass.

For normal, "short" outbursts, only a few percent of the stored gas accretes onto the central object: the thermal time scale of thin disk is short compared to the viscous time scale, and the cooling front that is launched from the outer edge of the disk almost as soon as the disk enters into outburst traverses the disk and reverts it back to quiescence. For disks that have been "filled" to a higher level with respect to $M_{\rm disk,\ max}$, the surface density in the outer disk can significantly exceed the critical surface density $\Sigma_{\rm min}$. In order for the cooling front to begin, however, the outer surface density $\Sigma(r_{\rm outer})$ must drop below $\Sigma_{\rm min}(r_{\rm outer})$. Disks in this state generate much longer outbursts, with slower "viscous" plateaus, because the entire disk must remain in its high, completely ionized state until enough mass has been lost onto the WD for the condition $\Sigma(r_{\rm outer}) < \Sigma_{\rm min}(r_{\rm outer})$ to be satisfied. The slow decay associated with a superoutburst is a direct reflection of the viscous time scale in the outer disk, whereas the subsequent faster decay reveals the thermal time scale. Although the decays of dwarf novae at a given orbital period are fairly uniform, and form the basis for the Bailey relation, the rise times show a greater variety, reflecting the fact the the outburst can be triggered anywhere in the disk (Cannizzo 1998b). Inside-out bursts tend to produce slow-rise times, whereas outside-in bursts produce fast rises (Cannizzo, Wheeler, & Polidan 1986).

Whitehurst (1988) discovered a hydrodynamical instability that can occur in the outer parts of accretion disks when the mass ratio $q = M_2/M_1$ is less than 1/4. For these extreme mass ratio systems, expected in CVs below the period gap if the secondary fills its Roche lobe, the outer part of the disk can lie beyond the point of 3:1 resonance with the binary period. The outer disk can then be excited by the inner Lindblad resonance (Lubow 1991ab), causing the global disk oscillation mode that is observed as common superhumps. Before the onset of the superhump oscillation, there are well-known spiral dissipation waves in the disk that are fixed in the co-rotating frame. Once the superhump oscillation begins, these spiral arms advance 180° every superhump cycle[7]. As a given arm passes between the two stars, it expands outward in the shallower potential, but as fluid in that arm compresses back into the disk as the disk is maximally distorted, viscous dissipation causes a peak in the photometric light curve (Simpson & Wood 1998). A secondary source of the superhump signal is caused by the variable distance the mass stream must fall from the L1 point to the edge of the non-axisymmetric, flexing disk. Because the outer disk is thought to expand during superoutburst, potentially beyond the 3:1 radius, this "tidal instability" model provides a natural explanation for superhumps. If the mass ratio is extreme enough, superhumps can also occur outside of superoutbursts because the disk can remained extended beyond the 3:1 radius, and therefore eccentric, even into quiescence. Osaki (1989ab) combined the accretion disk limit cycle model with Whitehurst's tidal instability model and proposed the "thermal-tidal" instability model (TTIM) for superoutbursts. This model posits that the presence of an eccentric precessing disk, triggered by the migration of gas beyond the 3:1 resonance radius, also leads to a greatly enhanced tidal torque acting on the disk. This ultimately contracts the outer disk and leads to a superoutburst. Thus in the TTIM one has the usual hysteresis relation between surface density and temperature in the disk, and also a hysteresis relation between the total angular momentum of the disk and the tidal torque acting on the outer disk. (The latter hysteresis is somewhat speculative.) This model was examined in detail and compared to the enhanced mass transfer model (EMTM) for superoutbursts by Ichikawa, Hirose, & Osaki (1993) and later workers, most recently Schreiber et al (2004).

[7] See, for example, www.astro.fit.edu/wood/visualizations.html.

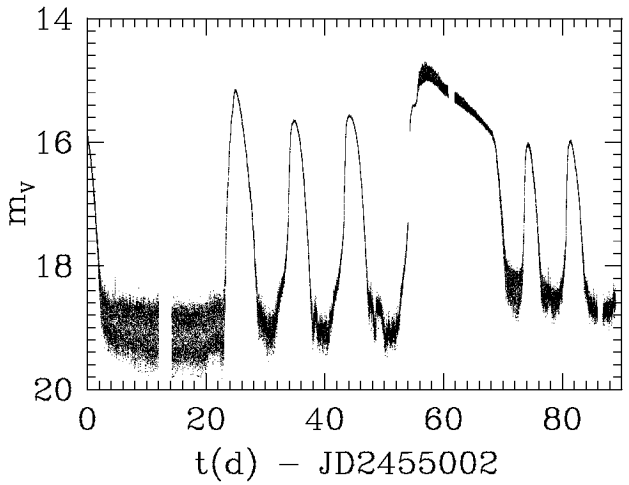

FIG. 1.— *Kepler* light curve of V344 Lyr over 89 d showing outbursts every ∼10 d, with one superoutburst and one failed normal burst. The flux is measured in e^- cadence^{-1}, where the cadence (time between integrations) is 1 m. The full time resolution is shown. To obtain visual magnitude, a correspondence of $m_V = 12$ to 10^7 e^- cadence^{-1} was adopted.

3. *KEPLER* LIGHT CURVE OF V344 LYR

Figure 1 shows the *Kepler* light curve of V344 Lyr. The observation window contains outbursts showing the sequencing SSSLSS, where S=short outburst and L=long outburst, i.e., a superoutburst. Based on photographic observations made by Hoffmeister (1966), Kato (1993) estimated that the cycle length for normal outbursts was 16±3 d. An estimate of this cycle length is difficult because the normal outbursts of V344 Lyr are short-lived and reach only to near $m_V = 16$. Using our five complete normal outbursts, we find that prior to the

TABLE 1
DURATION AND AMPLITUDE OF NORMAL OUTBURSTS

Outburst	Duration (day)	Amplitude (mag)
1	5.5	4.0
2	5.0	3.6
3	5.3	3.6
4	3.3	2.4
5	4.0	2.6

superoutburst, the cycle length is 9.6 d, while after the superoutburst it shortens to 7.2 d. The normal outburst amplitude and duration also changes from before (normal outbursts 1, 2, 3) to after (normal outbursts 4, 5) the superoutburst (Table 1). We also note that the level of quiescence is ∼0.5 mag higher after the superoutburst, indicating a larger contribution from the disk emission. Since the disk is a bit smaller and has less mass at this point (see Section 6), we believe that this brighter disk is due to it being hotter overall directly after the superoutburst.

The superoutburst lasted 17.6 d and reached a maximum amplitude of 4.2 mag. The decline of the superoutburst is close to linear (plotted as mag versus time, or exponential as flux versus time) from near day 57 until day 68, after which it falls rapidly (∼2 d) back to quiescence. During this part the decline rate is 0.083 mag d^{-1}, in good agreement with the value of 0.094 mag d^{-1} found by Kato (1993). The amount of time spent at $m_V \lesssim 16$ is ∼14 d, and the duration of the entire plateau is ∼12 d. The decay rate is ∼12 d mag^{-1}, therefore the plateau portion of the decay encompasses ∼1 mag – a dynamic range of ∼2.5, or slightly less than one $e-$folding (∼2.7×). There is also a ∼0.5 mag shoulder on the superoutburst rise lasting ∼1 d.

It is noteworthy that the fast decays of the normal outbursts and superoutburst have a faster-than-exponential shape (i.e., concave downward when plotted as magnitude versus time). S84 utilized the Bailey relation between the fast rate of decay in dwarf novae and their orbital period to constrain $\alpha_{\rm hot} \simeq 0.1-0.2$. The large errors associated with the AAVSO data were consistent with exponential decay. Cannizzo (1994) found that to account for the supposedly exponential decays, which correspond to the time during which a cooling front traverses the disk, α must vary weakly with radius ($\sim\propto r^{0.3}$). As we show later, the faster-than-exponential decays captured by *Kepler* in V344 Lyr negate this result and indicate that a constant α scaling with radius is consistent with the data.

For any dynamical system in which a variety of timescales contribute to a physical observable, in this case the flux from the accretion disk, the controlling time scale will be the slowest one. Since all the disk timescales – dynamical, thermal, and viscous – increase with radius, the time scale associated with the viscous plateau provides direct information about the viscous time scale $t_{\rm visc}$ at the outer edge of the disk.

Starting with a general theoretical expression from Frank, King, & Raine (2002) relating the locally defined viscous time to α, r, and accretion rate $\dot{M}$, King & Pringle (2009) estimate a local peak accretion rate during outburst as $\simeq 2M_{\rm disk,hot}/t_{\rm visc}$, where $M_{\rm disk,hot}$ is the mass of the hot disk which they estimate as $M_{\rm disk,\ min}$ times a factor of order unity, and derive a viscous time for the outbursting disk (see their eqn. [2])

$$t_{\rm visc} = 14 \ {\rm d} \ \alpha_{-1}^{-0.8} \ r_{10}^{0.48} \ m_1^{0.15} \qquad (3)$$

where $\alpha_{-1} = \alpha/0.1$, $r_{10} = r/(10^{10}$ cm), and $m_1 = M_1/M_\odot$. (The α in this context is the hot state value.) Within the viscous plateau portion of a superoutburst, the instigation and propagation of a cooling front at the outer edge is thwarted by virtue of excessive mass in the disk. The viscous time does not represent the duration of the outburst itself, but rather the time scale (approximately in d mag^{-1}) associated with the viscous plateau; it represents an $e-$folding time for the decrease of disk mass.

4. VISCOUS PLATEAUS IN DWARF NOVAE

The Bailey relation between the fast rate of decay of dwarf nova outbursts and orbital period corresponds to the time interval during which the cooling front traverses the disk. Some long dwarf nova outbursts have enough dynamic range in m_V that one can also use the slow decay portion, the viscous plateau, to infer an α value. These inferred values agree with those determined from the Bailey relation (Cannizzo 2001b, Cannizzo et al. 2002; King et al. 2007).

The decay rates associated with several dwarf novae exhibiting viscous plateaus have been fairly well established, and enable one to make a reasonable estimate of the decay rate expected in a system with the orbital period of V344 Lyr. As noted previously, for V344 Lyr one expects $t_{\rm visc} \simeq 14$ d mag^{-1}. The *Kepler* observation gives a decay rate within the superoutburst ∼12 d mag^{-1}. We associate this with the viscous time, which is basically an $e-$folding time for a perturbation to the $\Sigma(r)$ profile to be damped out. For a disk with a $\Sigma(r)$ profile approximating steady state, i.e., $\Sigma(r) \propto r^{-3/4}$, and for which the mass flow within the disk and onto the WD greatly exceeds the rate of mass addition feeding into the outer disk from the secondary star, the viscous time represents roughly a time for the mass of the disk to decrease by a factor e.

Thus for a given viscous plateau-type outburst, the ratio $t_{\rm plateau}/t_{\rm visc}$ represents the number of $e-$foldings by which the mass of the disk decreases due to accretion onto the central object. It is instructive to look at examples of viscous decays in several well-studied dwarf novae:

SS Cyg: Long outbursts in SS Cyg ($P_{\rm orb} = 6.6$ hr) have a duration of ∼10 d (Cannizzo & Mattei 1992). and the viscous time in the outer disk $t_{\rm visc} \approx 40$ d. Thus $t_{\rm plateau} \ll t_{\rm visc}$, and only a small fraction of the disk mass ∼0.2 is accreted onto the WD (Cannizzo 1993b=C93b).

U Gem: In the 1985 long outburst of U Gem ($P_{\rm orb} = 4.25$ hr), the decay rate during the viscous plateau was ∼26 d mag^{-1} over the ∼35 d of the burst (Cannizzo et al. 2002). Since $t_{\rm visc} \approx t_{\rm plateau}$, the disk mass decreased to about 0.3 of its initial value.

V344 Lyr: In the Aug 2009 superoutburst of V344 Lyr ($P_{\rm orb} = 2.06$ hr) shown in Fig. 1 the locally defined decay rate during the plateau remained constant at ∼12 d mag^{-1} over most of the ∼14 d of the burst, thus as with U Gem the disk mass remaining after the superoutburst would be about 0.3 of the initial amount.

WZ Sge: In the 2001 superoutburst of WZ Sge ($P_{\rm orb} = 81$ min), the locally defined decay rate during the plateau increased from ∼4 to ∼12 d mag^{-1} over the ∼20 d of the burst (Cannizzo 2001b). The fact that $t_{\rm plateau} \approx 3t_{\rm visc}$ means that only a few percent of the initial disk mass remained at the end of the superoutburst. (An alternative considered in the Discussion is that irradiation-induced enhanced mass overflow from the secondary star prolonged the superoutburst.)

In summary, one can readily find examples of known sys-

tems with viscous type outbursts in which the duration of the outburst itself is either greater than, less than, or about the same as the viscous time scale evaluated at the outer edge of the accretion disk. The actual course taken by a given system depends on the degree of overfilling of the disk in quiescence with respect to $M_{\rm disk,min}$.

5. NUMERICAL MODELING

Our numerical model is discussed extensively in C93b and subsequent papers. The basic strategy is the time dependent solution of two coupled differential equations, one giving the $\Sigma(r)$ evolution, and one the evolution of disk midplane temperature $T(r)$. Thus the disk is entirely unconstrained as regards deviations from steady state and thermal equilibrium. Many previous workers have presented time dependent calculations by solving these equations, or similar versions (e.g., S84; Lin, Papaloizou, & Faulkner 1985=L85; Mineshige & Osaki 1983, 1985=M85, Mineshige 1986=M86, 1987=M87; Pringle, Verbunt & Wade 1986=P86; Cannizzo et al. 1986=C86, C93b, 1994, 1998a, 2001a; Angelini & Verbunt 1989; Ichikawa & Osaki 1992; Ludwig & Meyer 1998; Hameury et al. 1998=H98, Menou, Hameury, & Stehle 1999, Buat-Ménard, Hameury, & Lasota 2001, Buat-Ménard, & Hameury 2002, Schreiber, Hameury, & Lasota 2004=S04).

Improvements in our code made since the original version include the provision for a variable outer disk radius, self-irradiation, and evaporation with various possible laws. The diffusion equation governing the evolution of surface density is given by (Lightman 1974, Pringle 1981)

$$\frac{\partial \Sigma}{\partial t} = \frac{3}{r}\frac{\partial}{\partial r}\left[r^{1/2} \frac{\partial}{\partial r}\left(\nu \Sigma r^{1/2} \right) \right], \tag{4}$$

where $\Sigma(r,t)$ is the surface density and ν is the kinematic viscosity coefficient,

$$\nu = \frac{2}{3}\frac{\alpha}{\Omega}\frac{\mathcal{R}T}{\mu}. \tag{5}$$

We follow the technique of Bath & Pringle (1981) in discretizing the $\Sigma(r,t)$ evolution equation.

The thermal energy equation governing the evolution of the midplane disk temperature $T(r,t)$ is given by

$$\frac{\partial T}{\partial t} = \frac{2(A-B+C+D)}{c_p \Sigma} - \frac{\mathcal{R}T}{\mu c_p}\frac{1}{r}\frac{\partial}{\partial r}(r v_r) - v_r \frac{\partial T}{\partial r}, \tag{6}$$

where the viscous heating

$$A = \frac{9}{8}\nu \Omega^2 \Sigma, \tag{7}$$

the radiative cooling

$$B = \sigma T_e^4, \tag{8}$$

$$C = \frac{3}{2}\frac{1}{r}\frac{\partial}{\partial r}\left(c_p \nu \Sigma r \frac{\partial T}{\partial r} \right), \tag{9}$$

and

$$D = \frac{h}{r}\frac{\partial}{\partial r}\left(r \frac{4acT^3}{3\kappa_R \rho}\frac{\partial T}{\partial r} \right). \tag{10}$$

Of the four terms appearing in the numerator of the first term of thermal energy equation, the first two A and B are fairly standard. The term C represents the radial heating flux due to turbulent transport, and D is that due to radiative transport. Previous workers have used varying forms of C and D. Some early studies adopted $C = D = 0$ (M83), $C = 0$ (L85), or a form of C not expressible as the divergence of a flux (M83, M86, C93b; see H98 for a critical discussion).

The local flow velocity v_r, which can vary enormously from inflow to outflow over the radial extent of the disk, depending on whether or not transition fronts are present, is given by

$$v_r = -\frac{3}{\Sigma r^{1/2}}\frac{\partial}{\partial r}\left(\nu \Sigma r^{1/2} \right), \tag{11}$$

where upwind differencing is implemented over the radial grid as follows:

$$\begin{aligned} s_a &= \nu_{i-1}\Sigma_{i-1} {r_{i-1}}^{1/2} \\ s_b &= \nu_i \Sigma_i {r_i}^{1/2} \\ s_c &= \nu_{i+1}\Sigma_{i+1} {r_{i+1}}^{1/2} \end{aligned} \tag{12}$$

$$\begin{aligned} q_- &= -\frac{3}{\Sigma_i {r_i}^{1/2}}\frac{s_b - s_a}{r_i - r_{i-1}} \\ q_+ &= -\frac{3}{\Sigma_i {r_i}^{1/2}}\frac{s_c - s_b}{r_{i+1} - r_i} \end{aligned} \tag{13}$$

$$\begin{aligned} &\text{if } \left(\frac{q_-}{q_+} > 0 \text{ and } q_- > 0 \right) \qquad (v_r)_i = \max(q_-, q_+) \\ &\text{if } \left(\frac{q_-}{q_+} > 0 \text{ and } q_- < 0 \right) \qquad (v_r)_i = \min(q_-, q_+) \end{aligned} \tag{14}$$

$$\begin{aligned} &\text{if } \left(\frac{q_-}{q_+} < 0 \text{ and } \frac{|q_-|}{|q_+|} > 1 \right) \qquad (v_r)_i = q_- \\ &\text{if } \left(\frac{q_-}{q_+} < 0 \text{ and } \frac{|q_-|}{|q_+|} < 1 \right) \qquad (v_r)_i = q_+. \end{aligned} \tag{15}$$

The scalings for the local maximum and minimum in the $\Sigma - T$ relation (from MM81)

$$\Sigma_{\rm max} = 444 \text{ g cm}^{-2}\ r_{10}^{1.1} m_1^{-0.37} \alpha_{c,-2}^{-0.7}, \tag{16}$$

where $\alpha_{c,-2} = \alpha_{\rm cold}/0.01$, and

$$\Sigma_{\rm min} = 44.4 \text{ g cm}^{-2}\ r_{10}^{1.1} m_1^{-0.37} \alpha_{h,-1}^{-0.7}, \tag{17}$$

where $\alpha_{h,-1} = \alpha_{\rm hot}/0.1$. The disk midplane temperatures associated with these extrema are

$$T(\Sigma_{\rm max}) = 5275 \text{ K}\ \alpha_{c,-2}^{-0.3}, \tag{18}$$

and

$$T(\Sigma_{\rm min}) = 35900 \text{ K}\ r_{10}^{0.064} m_1^{-0.02} \alpha_{h,-1}^{-0.16}. \tag{19}$$

The equilibrium temperature scalings for the stable branches are given in C93b (taken from Cannizzo & Wheeler 1984). During transitions when the local disk temperature lies between the values associated with the local maximum and minimum in surface density, $T[\Sigma_{\rm max}(r)] < T(r) < T[\Sigma_{\rm min}(r)]$, we use a logarithmic interpolation to obtain the local α value,

$$\log_{10}\alpha(r) = \log_{10}\alpha_{\rm cold} + f, \tag{20}$$

where

$$f = \frac{T - T(\Sigma_{\rm max})}{T(\Sigma_{\rm min}) - T(\Sigma_{\rm max})}(\log_{10}\alpha_{\rm hot} - \log_{10}\alpha_{\rm cold}). \tag{21}$$

In tests we also consider a logarithmic interpolation factor f introduced by H98,

$$f = \left[1 + \left(\frac{T_0}{T}\right)^8\right]^{-1} (\log_{10}\alpha_{\rm hot} - \log_{10}\alpha_{\rm cold}), \quad (22)$$

as well as a linear interpolation

$$\alpha(r) = \alpha_{\rm cold} + \frac{T - T(\Sigma_{\rm max})}{T(\Sigma_{\rm min}) - T(\Sigma_{\rm max})}(\alpha_{\rm hot} - \alpha_{\rm cold}). \quad (23)$$

In calculating the effects of the tidal torque from the secondary we follow Smak (1984) and later workers who used a formalism developed by Papaloizou & Pringle (1977) in which the tidal torque varies as the fifth power of radius. This leads to a depletion in disk material

$$\frac{\partial\Sigma}{\partial t} = -c_1\omega\frac{\nu\Sigma}{2\pi j_s}\left(\frac{r}{a}\right)^5, \quad (24)$$

where ω is the orbital angular frequency $2\pi/P_{\rm orb}$, the orbital separation is a, and the specific angular momentum $j_s = (GM_1 r)^{1/2}$. We do not reset the value of c_1 during the course of a run as in the TTIM. Ichikawa & Osaki (1994) presented detailed calculations of the strength of the tidal torque versus distance at large radii within the disk and found that the power law ($\propto r^5$) determined by Papaloizou & Pringle is only valid at one radial location in the outer disk; further out the torque relation steepens considerably, approaching infinite slope at the last non-intersecting orbit. Therefore in some sense the more naive "brick wall" condition for the outer edge used by C93b and other workers might be more descriptive. Regardless of which prescription is used, if the parameters associated with the outer edge are not manipulated during the run, the detailed treatment is not important to the overall model. Using a different end point treatment would result in slightly different optimal parameters.

Given a disk temperature T and surface density Σ, the disk semithickness h and density ρ are determined from vertical hydrostatic equilibrium to yield

$$h = \frac{P_r + \sqrt{P_r^2 + c_2 c_3}}{c_2}, \quad (25)$$

where

$$c_2 = \Sigma\Omega^2, \quad (26)$$

$$c_3 = \Sigma\frac{\mathcal{R}T}{\mu}, \quad (27)$$

the radiation pressure

$$P_r = \frac{1}{3}aT^4, \quad (28)$$

and the density

$$\rho = \frac{\Sigma}{2h}. \quad (29)$$

To determine the computational time step, we take

$$\Delta t = f_t \min\left[\min_i\left(\frac{\partial\ln\Sigma_i}{\partial t}\right)^{-1}, \min_i\left(\frac{\partial\ln T_i}{\partial t}\right)^{-1}\right], \quad (30)$$

where $\min_i$ refers to the minimum over all grid points i, and f_t is a small number between $1/80$ and $1/640$. The quantities $\partial\ln\Sigma_i/\partial t$ and $\partial\ln T_i/\partial t$ are evaluated using the evolution equations.

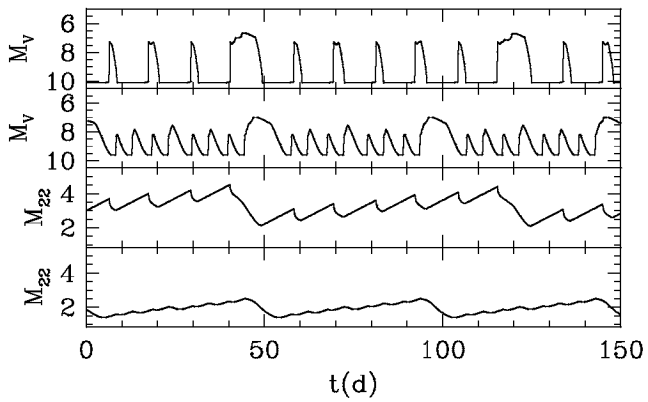

FIG. 2.— The effect of using a logarithmic interpolation (eqn. [21]) versus a linear one (eqn. [23]) for α. For these runs $N = 800$ and $f_t = 1/160$. Shown are the light curves for the logarithmic case (*top panel*) and the linear case (*second panel*), as well as the accompanying disk masses (*third and fourth panels*). The disk masses are in units of 10^{22} g.

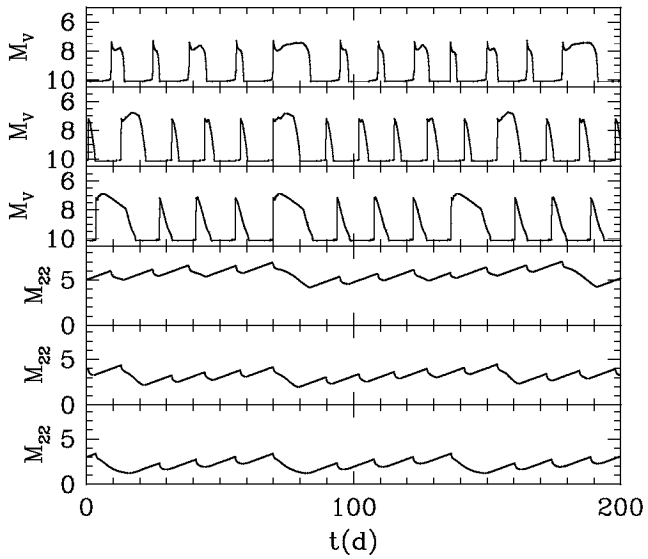

FIG. 3.— The effect of using the H98 logarithmic factor f (eqn. [22]). For these runs $N = 800$ and $f_t = 1/160$. Shown are the light curves for $T_0 = 25000$ K (*top panel*), 18750 K (*second panel*), and 12500 K (*third panel*), as well as the accompanying disk masses (*fourth through sixth panels*). The disk masses are in units of 10^{22} g.

6. RESULTS

To calculate the long-term light curves from our numerical trials, we assume local Planckian flux distributions for each annulus, and in each time step integrate over the radial profiles of effective temperature. We compute the absolute Johnson V-band magnitude, assuming a face-on disk. A reasonable inclination $i \simeq 45°$ would dim the disk by $\sim$0.4 mag. After some experimentation, we found a set of parameters that reproduces approximately the overall pattern of supercycle and short outbursts. We take a central $0.6M_\odot$ WD accretor, an inner disk radius $r_{\rm in} = 2\times10^9$ cm, and a maximum outer disk radius $r_{\rm out} = 10^{10}$ cm, a mass feeding rate into the outer disk $\dot{M}_T = 2\times10^{-10}M_\odot$ yr^{-1}, and α values $\alpha_{\rm cold} = 0.0025$

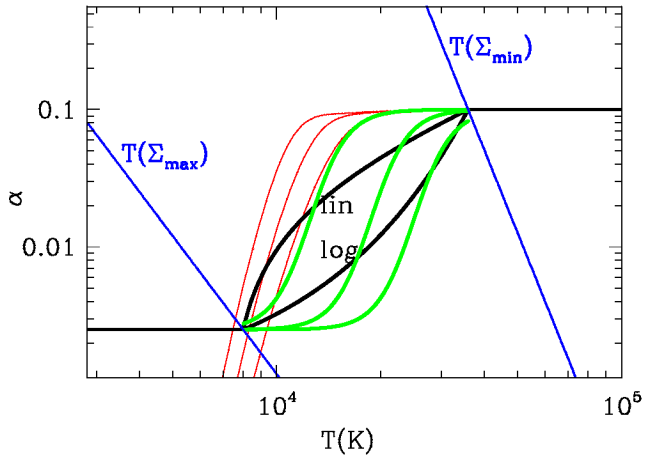

FIG. 4.— Shown are the different $\alpha_{\rm cold} - \alpha_{\rm hot}$ interpolations. The blue lines show the scalings for $T(\Sigma_{\rm max})$ and $T(\Sigma_{\rm min})$. The black curves indicate the linear (eqn. [23]) and logarithmic (eqn. [21]) interpolations. The green curves show the H98 scaling (eqn. [22]), where the three curves (left to right) represent $T_0 = 25000$ K, 18750 K, and 12500 K. The three red curves show a measure of the partial ionization; they are the relative contribution of electron pressure to total pressure as shown in Fig. 16 of C93b, for ρ(g cm^{-3})= 10^{-8}, 10^{-7}, and 10^{-6} (left to right). The values given in C93b have been multiplied by $2\alpha_{\rm hot}$ to take into account the fact that (1) $P_e/P \rightarrow 0.5$ in the limit of complete ionization, and (2) in the high temperature limit $\alpha \rightarrow \alpha_{\rm hot} = 0.1$.

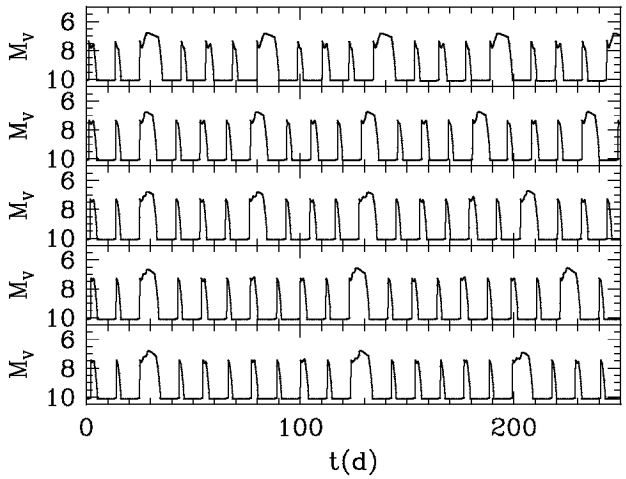

FIG. 5.— Long-term model light curves for $N = 100$, 200, 400, 800, and 1600. For these runs $f_t = 1/640$. The light curves have been aligned so that a superoutburst begins at $t = 25$ d.

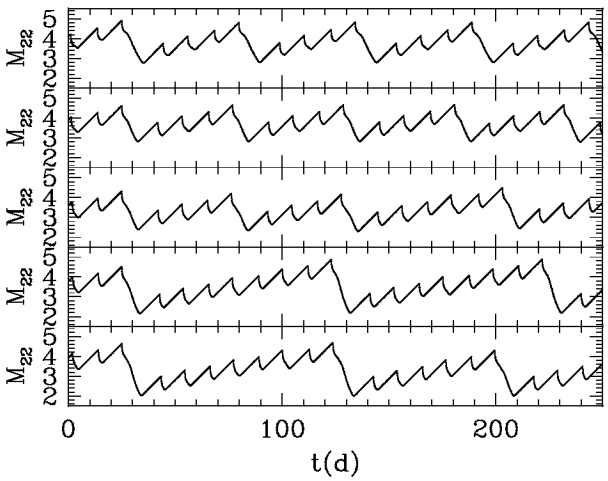

FIG. 6.— The disk mass in units of 10^{22} g accompanying the light curves shown in Fig. 2.

and $\alpha_{\rm hot} = 0.1$. We use the α interpolation given by eqn. (21). As regards the inner disk radius, the value for $r_{\rm inner}$ is larger than the WD itself; if we take $r_{\rm inner} \simeq r_{\rm WD}$, we tend to get far fewer short outbursts between two successive superoutbursts. This hint of a large inner radius may have some observational support in the SU UMa systems (e.g., Howell et al. 1999). The ratio $\alpha_{\rm cold}/\alpha_{\rm hot} = 40$ is about 10 times greater than commonly used in dwarf nova calculations. The mass transfer rate from the secondary $\dot{M}_T$ is twice the nominal value $10^{-10} M_\odot$ yr^{-1} found from evolutionary calculations of cataclysmic variables below the period gap where the evolution is driven predominantly by gravitational radiation (e.g., Kolb, King, & Ritter 1998; Howell, Nelson, & Rappaport 2001). When one takes into account the ∼20% depletion of the disk mass accompanying each of the short (normal) outbursts, however, the effective rate of accumulation of mass in the disk between successive superoutbursts decreases from $2 \times 10^{-10} M_\odot$ yr^{-1} to $\sim 0.3 \times 10^{-10} M_\odot$ yr^{-1}. In our models, ∼40−60% of the disk mass is accreted during a superoutburst.

In using a complicated numerical model, it is important to carry out testing to gain an understanding of systematic effects:

6.1. *Interpolation between* $\alpha_{\rm cold}$ *and* $\alpha_{\rm hot}$

Figure 2 shows the effect of using a log versus a linear interpolation for the α value between $\alpha_{\rm cold}$ and $\alpha_{\rm hot}$. The linear interpolation leads to smaller amplitude outbursts with little or no quiescent intervals. The decays are also much slower, and concave upwards when plotted as mag versus time (i.e., with a functional form that is slower-than-exponential). Figure 3 shows the effect of using the H98 interpolation. H98 adopted the constant $T_0 = 25000$ K in their scaling; we also look at smaller values 18750 K and 12500 K. The smaller T_0 values produce superoutbursts which have the recognizable plateau and subsequent fast decay, but for the $T_0 = 12500$ K run the fast decays are slower-than-exponential.

Figure 4 depicts the different interpolations as well as parameterizations of the fractional ionization ξ. The MRI is thought to mediate the strength of α through turbulent transport, and the effect of shearing on the weak magnetic field embedded in the gas is more efficient as ξ increases. The H98 scaling for $T_0 = 12500$ K does a reasonable job in approximating the $\rho = 10^{-6}$ g cm^{-3} curve for ξ, and may be more physical than the other scalings.

6.2. *Number of Grid Points N*

Early time dependent accretion disk limit cycle studies were concerned mainly with showing the ability of the disk, under the conditions of an imposed limit cycle in each annulus, to undergo collective, global oscillations in which a major part

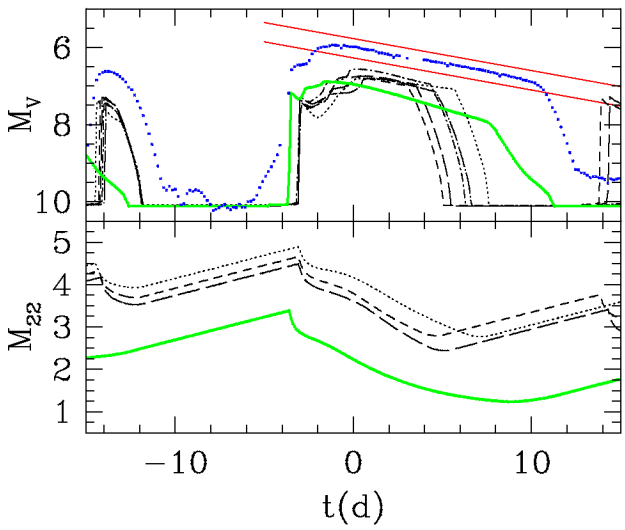

FIG. 7.— Model light curves showing the detail of a superoutburst from each panel of Fig. 5 for $N = 100$ (*dotted*), 200 (*short dashed*), 400 (*long dashed*), 800 (*short dash-dotted*), and 1600 (*long dash-dotted*). The green curve shows a superoutburst from the $T_0 = 12500$ H98 scaling light curve of Fig. 3. For comparison the averaged *Kepler* data for V344 Lyr is shown (blue), where the original $\Delta t = 1$ min cadence has been block-averaged to $\Delta t = 4$ hr. The two slanted red lines indicate a decay slope of 12 d mag^{-1}. The second panel shows the disk mass (in 10^{22} g) as in Fig. 3.

of the disk participated. The total numbers of grid points N was small and the comparison with observational data minimal (e.g., $N = 20 - 25$: S84; $N = 35$: L85; $N = 22 - 44$: M85; $N = 17$: M86; $N = 40$: P86; $N = 44$: C86). One can see obvious irregularities in many of the early light curves which are characteristic of numerical instability. C93b undertook the first detailed investigation regarding the number of grid points, and found that at least several hundred were required to obtain reliable light curves. H98 utilized both uniform and adaptive mesh codes to study the properties of the transition fronts, and found a requirement of $N \gtrsim 800$ for a uniform-equivalent mesh to resolve the fronts adequately.

Figure 5 shows long term light curves for models with $N = 100$ to 1600 grid points. The rise times we calculate, both for the normal and superoutbursts, are too fast. In addition, our outbursts are too faint by ∼0.5 mag. A nominal inclination $i \simeq 45°$ would make our disks dimmer by ∼0.4 mag and increase the discrepancy to ∼1 mag. The shoulders on the rise to superoutburst in the models have more structure than the shoulder in the observed superoutburst. The shoulders are caused by the strong spreading of material out of the annulus in which the instability starts. This results in a brief reversal in the increase of the local disk temperature. The rate of brightening in V is set by a combination of the widening radial extent of the unstable annulus, and the increase or decrease of temperature within the annulus. The subsequent rise after the shoulder is due to the full radial extent of the disk out to the outer edge making a transition to the hot state. In contrast, for the short (normal) outbursts, not enough disk mass has accumulated at larger radii by the time of the outburst to support the heating transition front propagating to large radii, therefore the heating front stalls at some $r < r_{\rm outer}$ and is reflected as a cooling front, leading to pointy maxima rather than viscous plateaus.

For smaller N one sees spuriously long and slowly decaying superoutbursts, and only 3 short outbursts between two successive superoutbursts. For $N \gtrsim 800$ the pattern asymptotes to LSSSSSSSLSSSSSSS... The decrease in superoutburst duration from $N = 100$ to $N = 200$ is consistent with the trend noted by C93b. Figure 6 indicates the variations in accretion disk mass accompanying each panel in Fig. 5. Figure 7 shows a detail of one superoutburst from each panel in Fig. 5. For comparison we also plot the V344 Lyr data, where $D = 620$ pc was assumed in converting to absolute magnitude (found by Ak et al. 2008 using a period-luminosity relation). There is a slight increase in superoutburst duration from $N = 200$ to $N = 800$ due to the fact that more mass accumulates as the supercycle lengthens. In addition, the shoulder in the light curve also becomes longer. For the highest N run the duration of the superoutburst is still shorter than that seen in V344 Lyr, while the shoulder is too long. The superoutburst calculated using the H98 scaling with $T_0 = 12500$ K better reproduces the observed duration of the V344 Lyr superoutburst, and also has a shorter shoulder with less structure than the other calculations. However, it suffers from a rise time that is too short, and the fast decay is now slower-than-exponential. Also, the viscous decay rate, which has been optimized to the observed value using the eqn. (21) scaling, is now too fast.

6.3. *Thermal Energy Equation*

Considering the many forms of the thermal energy equation used by previous workers, and the potential limitations of employing a one-dimensional hydrodynamical formalism, we now look at the effects of switching off various terms in the thermal energy equation in an attempt to ascertain the relative importance of each term. Figure 8 shows the effect of setting equal to zero: (i) C, (ii) D, (iii) C and D, (iv) the first advective term in eqn. (6), and (v) the second advective term in eqn. (6). In the $C = 0$ run one sees a rounded superoutburst and only three short outbursts between two superoutbursts. The (radiative) D term is less influential, as the superoutburst profile is relatively unchanged from the first panel. Setting $C = D = 0$ produces a single dip in the rise to superoutburst, and a longer viscous plateau (i.e., exponential decay). The first advective term appears to be of comparably minimal importance as the D term; i.e., the omission of either has a negligible effect. The second advective term is the most influential of all terms examined: without it one has much longer superoutbursts – about 70% of the accumulated disk mass is accreted, which is about the same as in V344 Lyr. However, the viscous plateau still comprises less than half of the superoutburst, rather than the $\gtrsim 90\%$ seen in V344 Lyr.

6.4. *Detuning of Optimal Parameters*

There is a complicated interplay between the different parameters that enter into the overall results. In an effort to understand the effect each parameter has, we look at the effect of introducing a slow change into $\alpha_{\rm cold}$, $\alpha_{\rm hot}$, and $\dot{M}_T$. Figure 9 shows the resultant variations in the light curves and disk masses. The primary effect of increasing these parameters is to shorten the recurrence times. Figure 10 shows the effect of varying the inner disk radius. For smaller inner disk radii, one has a larger dynamic range in $r_{\rm outer}/r_{\rm inner}$ and as a result there tends to be a more complete emptying of the disk during outbursts, and therefore less of a tendency to have a series of short outbursts leading up to a superoutburst. The net in-

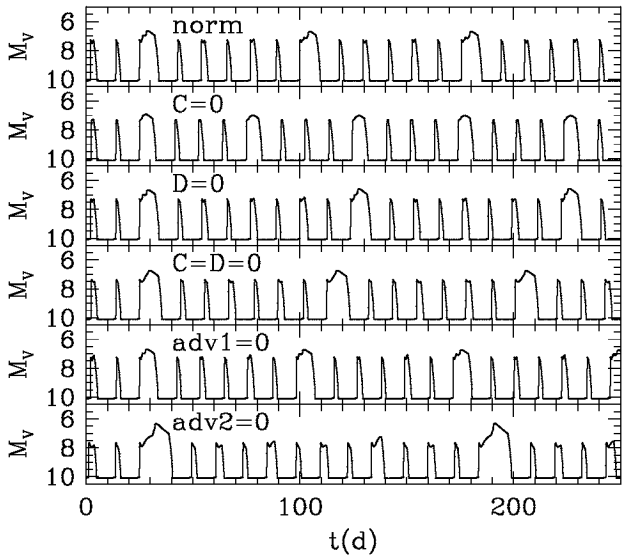

FIG. 8.— The effect of turning off different terms in the energy equation. For these runs $N = 800$ and $f_t = 1/160$. Shown are light curves using: the full equation (*top panel*), the turbulent transport $C = 0$ (*second panel*), the radiative transport $D = 0$ (*third panel*), both $C = 0$ and $D = 0$ (*fourth panel*), the first advective term set to zero (*fifth panel*), and the second advective term set to zero (*sixth panel*).

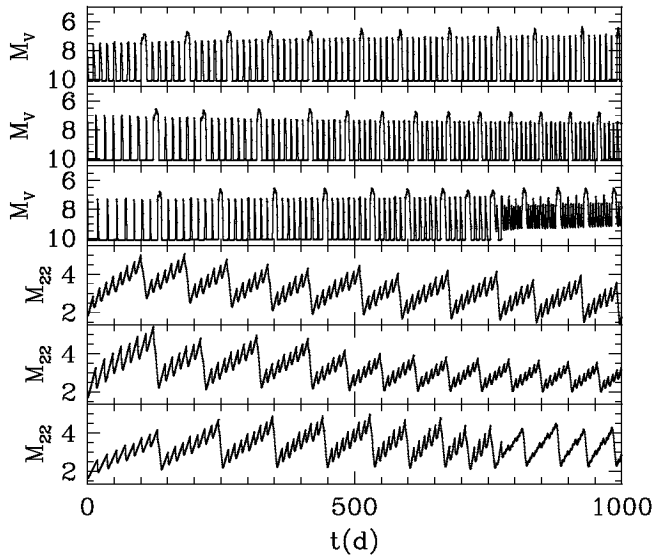

FIG. 9.— The effect of introducing a slow change into a given parameter, increasing the value linearly from half to twice its optimal value. For these runs $N = 800$ and $f_t = 1/160$. The six panels show the resultant light curves for $\alpha_{\rm cold}$ (*top panel*), $\alpha_{\rm hot}$ (*second panel*), and $\dot{M}_T$ (*third panel*). Also shown are the accompanying variations in disk mass, again in units of 10^{22} g (*fourth through sixth panels*).

teraction among all the model parameters is such that the observed sequencing for V344 Lyr is roughly reproduced with $r_{\rm inner} \simeq 2 \times 10^9$ cm. Figure 11 shows the effect of varying the outer disk radius. For larger $r_{\rm outer}$ values not only does the number of short outbursts increase, but also the shape of the superoutburst distorts significantly from the viscous plateau shape.

6.5. *Relevance of Results to the V344 Lyr light curve*

No one light curve we have shown reproduces all features of the observed light curve shown in Fig. 1. For instance, there is an atypically long quiescent period at the beginning of the observed light curve. Figure 9 in which we vary $\alpha_{\rm cold}$, $\alpha_{\rm hot}$, and $\dot{M}_T$ shows that if any one of these parameters were anomalously small, that could delay an outburst. Also, the pre-superoutburst normal outbursts are brighter than the post-superoutburst normal outbursts, and the pre-superoutburst quiescent level is fainter than the post-superoutburst quiescent level. As noted earlier, the disk instability model is ill-equipped to make any statement about the quiescent state, but Figure 9 again shows several possibilities. For instance, if $\dot{M}_T$ were elevated for a while after the superoutburst, that could lead to crowding of the short outbursts, and an increase in the quiescent level. There may be other causal relations among $\alpha_{\rm cold}$, $\alpha_{\rm hot}$, and $\dot{M}_T$, which are important.

The primary interpolation scheme we considered, given in eqn. (21), has clear problems in making good superoutbursts. The model superoutbursts have shoulders which comprise about a third to half of the total viscous plateau, rather than the $\sim$10% observed. However, for the H98 scaling with $T_0 = 12500$, the shoulders are appropriately short, $\sim$2 d, and the viscous plateaus much longer. The rate of decay of the viscous plateau is too fast, but that is because the input parameters have been optimized for the scaling given in eqn. (21).

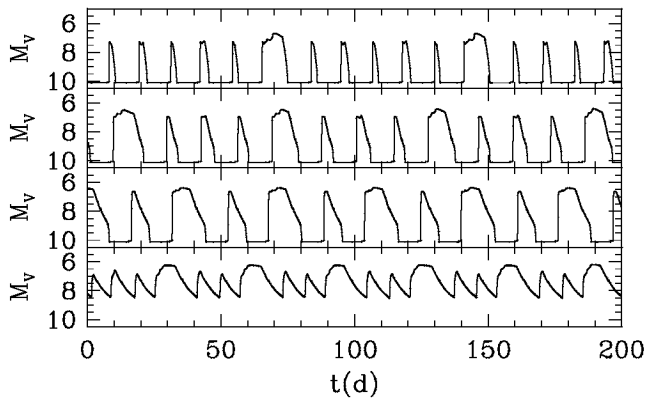

FIG. 10.— The effect of the inner disk radius. For these runs $N = 800$ and $f_t = 1/160$. The four panels show the resultant light curves for $r_{\rm inner} = 2 \times 10^9$ cm (*top panel*), 1.5×10^9 cm (*second panel*), 1×10^9 cm (*third panel*), and 0.5×10^9 cm (*fourth panel*).

7. DISCUSSION

In contrast to the thermal-tidal instability of Osaki (Ichikawa & Osaki 1992, 1994; Ichikawa, Hirose, & Osaki 1993) in which the tidal torque is artificially enhanced by a factor of 20 when the outer disk expands beyond the point of 3:1 resonance with the orbital period, our detailed modeling shows that the regular and superoutbursts can produced with a constant set of parameters. In retrospect, one may legitimately question the motivation for the increased tidal torque accompanying the expansion of the disk, considering that the ultimate driving force behind the tidal torque is the gravitational field of the secondary, which remains unchanged. We argue that the superoutbursts seen in the SU UMa systems

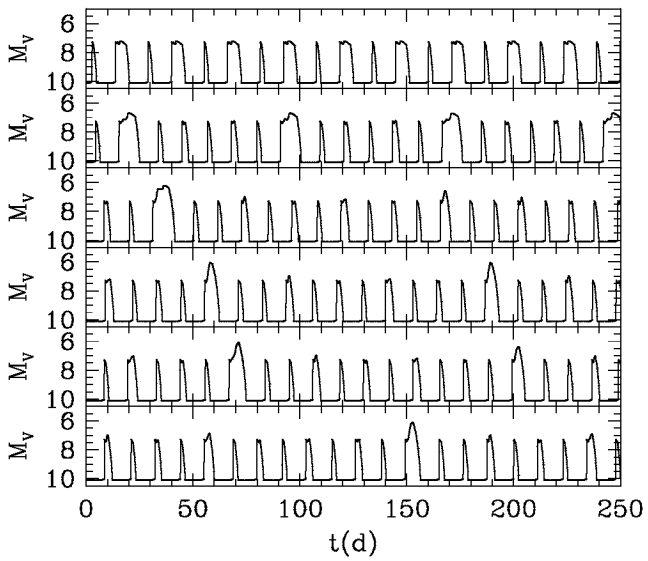

FIG. 11.— The effect of the outer disk radius. For these runs $N = 800$ and $f_t = 1/160$. The six panels show the resultant light curves for $r_{\rm inner} = 0.8 \times 10^{10}$ cm (*top panel*), 1.0×10^{10} cm (*second panel*), 1.25×10^{10} cm (*third panel*), 1.5×10^{10} cm (*fourth panel*), 1.75×10^{10} cm (*fifth panel*), and 2.0×10^{10} cm (*sixth panel*).

may be viewed as an extension of the long outbursts seen in DNe above the period gap, such as U Gem and SS Cyg (Cannizzo & Mattei 1992, 1998; C93b). Continued monitoring of V344 Lyr should reveal the stability of the long term sequencing, i.e., variations in the number of shorts sandwiched between two longs.

Our testing has delineated a range of allowable parameters:

(1) The logarithmic interpolation for α produces well-separated outbursts, with concave downward decays, as observed. The linear interpolation produces outbursts with minimal quiescence and concave upward decays. Given the physical underpinnings of the MRI, the logarithmic interpolation is better motivated since the MRI strength should depend on the partial ionization fraction, which is a strongly increasing function of temperature.

In terms of the superoutburst, the H98 scaling with $T_0 = 12500$ K produces the best overall results. The shoulder feature only persists ~ 2 d, as observed, and the viscous plateau is longer. About 70% of the stored mass is accreted. The main deficiencies are that the fast decay (i.e., that following the viscous plateau) is slower-than-exponential, and the rise times are too fast (as with the other calculations).

(2) The minimum number of grid points necessary is $\gtrsim 10^3$ (in accord with C93b and H98). Even for high N, the sequencing is not perfectly stable.

(3) Of the terms entering into the thermal energy equation, the radial viscous transport term C and the second advective term, $v_r(\partial T/\partial r)$ appear to be the most important. The radial radiative flux term D and the first advective term, involving $\partial(rv_r)/\partial r$, are of lesser importance.

(4) The values for $\alpha_{\rm cold} = 0.0025$, $\alpha_{\rm hot} = 0.1$, and $\dot{M}_T = 2\times10^{-10} M_\odot$ yr^{-1} are mandated by the observed spacing and duration of short outbursts and the superoutburst. Increasing their values decreases the outburst time scales.

(5) The values $r_{\rm inner}$ and $r_{\rm outer}$ strongly mediate the number of short outbursts between two superoutbursts. For $N = 800$ and $f_t = 1/160$ we have $\sim$5 shorts between two longs for $r_{\rm inner} = 2 \times 10^9$ cm, or $\sim 3R_{\rm WD}$ for $M_{\rm WD} = 0.6M_\odot$. Observations by Howell et al. (1999) seem to favor an evacuated inner disk. Several possibilities are discussed by these workers, including the possibility of weak polars in the SU UMa systems. The outbursts in our models are triggered at intermediate disk radii, therefore the outer disk radius has minimal effect on the outburst recurrence times and durations. Increasing $r_{\rm outer}$ from 1×10^{10} cm to 2×10^{10} cm increases the number of shorts between to successive longs, and also distorts the profile of the superoutburst.

Menou (2000) attempted a completely self-consistent calculation in which the local value of the fractional ionization parameter ξ (determined from density and temperature) set the level of the MRI instability. The model started with a transition to outburst state, and then continued into outburst and back to quiescence. When the disk started to cool, a runaway transition occurred such that the disk cooled to absolute zero, effectively terminating the simulation. This came about basically because ξ depends exponentially on temperature, through the Saha equation, whereas the level of turbulent transport, determined from the MRI, depends linearly. It has been recognized that, due to the very low ξ values near disk midplane in quiescence in the standard models, the standard S$-$curve relation between Σ and T is probably a convenient approximation for a much more complicated situation. In other words, there must be some additional angular momentum transport mechanism operating in quiescence. Alternatively, the quiescent disk may be essentially inviscid, and it may be the onset of finite and large partial ionization near the midplane, due to the accumulated effect of irradiation on the quiescent disk that is in fact the trigger for dwarf nova outbursts (Gammie & Menou 1998). This is sometimes referred to as the "dead zone" model (Gammie 1996) to encapsulate the fact that the quiescent disk may consist of an "active", irradiated layer with some radial mass flow that sandwiches a relatively inert inner core. In view of these considerations, and the current lack of predictive power in these type of models, we view our adoption of a small $\alpha_{\rm cold}$ for an SU UMa system as a necessary expedient which may have little physical significance. It is more noteworthy that $\alpha_{\rm hot}$, which is dictated by the outburst properties, is in line with that determined from dwarf novae in general (King, Pringle, & Livio 2007). This is consistent with the notion that the MRI becomes fully active in outburst disks where $\xi \approx 1$ and reaches a well-defined saturation level, equivalent to $\sim$10% of the gas pressure, in the $\alpha-$ disk parlance (Balbus & Papaloizou 1999).

With $\alpha_{\rm hot} = 0.1$, we match the rate of decay of the viscous portion of the superoutburst, and also find a $\sim$0.5 mag shoulder on the rise to superoutburst. It is not clear why previous detailed time dependent modelers did not find this shoulder (e.g., S04). The main deficiency in the models we present is our failure to obtain a sufficiently long viscous plateau on the superoutburst. The observed plateau has a decay rate of $\sim$12 d mag^{-1} and lasts for $\sim$12 d, which corresponds to ~ 1 $e-$folding in the decay of the disk mass, meaning about 60% of the disk mass should be accreted. Our viscous plateau lasts $\sim$6$-$8 d, with proportionally less mass accreted. The values for $\alpha_{\rm cold}$, $\alpha_{\rm hot}$, and $\dot{M}_T$ have already been optimized to get the supercycle and normal cycle periods of $\sim$100 d and $\sim$10 d,

respectively. One suspects that the scalings for $\Sigma_{\rm max}(\alpha_{\rm cold})$ and $\Sigma_{\rm min}(\alpha_{\rm hot})$ are too simplistic and fail to take into account the actual disk physics, particularly that of the quiescent state, which is presently unknown. One could envision introducing an ad hoc multiplicative parameter for $\Sigma_{\rm max}$, for instance to artificially enhance it, but then one would have to re-adjust all the other parameters, in particular increasing $\dot{M}_T$ which is already uncomfortably large. In view of these considerations we consider our experiment moderately successful in that we are able to reproduce the duration of the viscous plateau within a factor of two in an over-constrained system for which $\alpha_{\rm cold}$ and $\alpha_{\rm hot}$ have already been determined by the outburst properties.

What about having enhanced mass transfer from the secondary prolong the duration of the superoutburst? Smak (2004) presented observational evidence for enhanced hot spot brightness near superoutburst maxima which he interpreted as being due to enhanced mass transfer brought about by the strong irradiation of the secondary. Osaki & Meyer (2003) presented a theoretical study of the effects of irradiation on the photosphere of the secondary star in SU UMa systems and concluded that mass transfer could not be enhanced by a significant amount. S04 presented detailed calculations of both the TTIM and the EMTM, and in the end concluded that the EMTM was favored. Their arguments are rather general, however, and they state "... we have not proven the EMTM to be correct nor the TTIM not to work." Both models have a number of free parameters in addition to those already present in the standard limit cycle model. For the TTIM one has the time delay between the attainment of the 3:1 radius by the outer disk edge and the onset of enhanced tidal torque, in addition to the functional form and amplitude associated with the increase. Similarly the EMTM has as free parameters the degree of augmentation of $\dot{M}_T$ during superoutburst, as well as its functional form with time.

Our calculations, which are based solely on the standard limit cycle model, give alternating series of many short outbursts followed by a superoutburst, but the superoutburst durations are too short. This would appears to leave open the possibility for enhanced mass transfer, but we are unable to give it a strong endorsement for several reasons. The primary reason is that the α interpolation is uncertain, given that we do not currently have an ab initio theory for α based on the MRI, and this weak point in the theory leads to a larger uncertainty in the light curves than the other systematic effects. The MRI is a powerful instability for which the most rapidly growing wavenumbers in a thin disk have growth rates of $\sim 0.75\Omega$, a factor of $\sim 10^6$ in < 3 rotation periods (Balbus & Hawley 1991). One rotation period in the outer disk is $2\pi\Omega^{-1} \simeq 700$ s $r_{10}^{3/2}$, which is much faster than any time scale associated with the outbursts. Therefore "α" should adjust itself rapidly to a value in accord with the local physical conditions (i.e., ξ) in the disk at any given time. The H98 scaling with $T_0 = 12500$ may therefore represent the best physically motivated of the interpolation scalings we investigate, and it also does the best job at reproducing the main features of the superoutburst - its long duration, and the short ($\sim$2 d) shoulder feature.

In addition, there may be a problem with the viscous decay in the EMTM: The V344 Lyr superoutburst maintained a closely exponential decay over $\sim$1 mag, whereas our models as well as others reveal a definite slower-than-exponential trend (i.e., concave upward when plotted as magnitude versus time) in viscous plateaus covering that much dynamic range. Although the viscous decays can be lengthened in the EMTM, they tend to have noticeable deviations from exponentiality, in contrast to the V344 superoutburst. The fact that the short orbital period system WZ Sge did show a deviation from exponentiality in its 2001 outburst, which also spanned a greater dynamic range than in the V344 Lyr superoutburst ($\sim$ 2 mag versus $\sim$1 mag), may indicate that irradiation-induced enhanced mass transfer is a factor at much shorter orbital periods than for V344 Lyr. In addition, the amplitude of the $\sim$0.5 mag shoulder on the rise to superoutburst is roughly matched in our calculations; with enhanced mass transfer the shoulder amplitude is too great ($\gtrsim$ 1 mag). We consider it fortunate that we have matched the decay as well as we have since the scalings for the extrema in the limit cycle model, in particular $\Sigma_{\rm max}(\alpha_{\rm cold})$, are most probably gross simplifications to a more complicated situation that is currently beyond our understanding.

8. CONCLUSION

We have presented detailed time dependent calculations of the accretion disk limit cycle mechanism with application to the *Kepler* light curve of V344 Lyr. We find that the standard disk instability model is able to account for the mixture of normal and superoutbursts with a minimal amount of fine-tuning. Therefore we argue that both the thermal-tidal model and the enhanced mass transfer model with their additional free parameters, considered in detail by Schreiber et al (2004), are unnecessary. One can in some sense view the alternation of many successive short outbursts with a superoutburst as an extensive of the pattern of short and long outbursts seen in the longer orbital period systems such as U Gem and SS Cyg; for SU UMa parameters one has many more short outbursts between two longs than in a system like SS Cyg, which exhibits LSLSLS... most of the time (Cannizzo & Mattei 1992). For our standard model parameters, we find that $\gtrsim$ 800 grid points are required for numerical stability, with a resulting pattern in which 5$-$7 short outbursts occur between two successive superoutbursts (for $f_t = 1/640$). Having constrained $\alpha_{\rm cold}$ and $\alpha_{\rm hot}$ so as to produce the overall recurrence time scales of short outbursts and superoutbursts, there are several obvious deficiencies: the rise times of all outbursts are too fast, the superoutburst duration is too short, and the duration of the shoulder is too long and has an extra scalloped-out feature prior to the observed shoulder. However, the more physically motivated H98 scaling with $T_0 = 12500$ does a better job on making superoutbursts with minimal shoulders as observed, lasting $\sim$2 d, and also longer viscous plateaus. Overall, our outbursts are too faint by $\sim$1 mag for an intermediately inclined disk. It may be that the assumed distance 620 pc for V344 Lyr (from Ak et al. 2008) is slightly too large.

We thank James Bubeck (under the SESDA II contract) at Goddard Space Flight Center for assistance in providing local computational resources, and Marcus Hohlmann and Patrick Ford from the FIT High Energy Physics group and the Domestic Nuclear Detection Office in the Dept. of Homeland Security for making additional resources on a Linux cluster available.

We acknowledge the contributions of the entire *Kepler* team.

REFERENCES

Ak, T., Bilir, S., Ak, S., & Ezer, Z. 2008, New Astr, 13, 133
Angelini, L., & Verbunt, F. 1989, MNRAS, 238, 697
Balbus, S. A., & Hawley, J. F. 1991, ApJ, 376, 214
Balbus, S. A., & Hawley, J. F. 1998, Rev Mod Phys, 70, 1
Balbus, S. A., & Papaloizou, J. C. B. 1999, ApJ, 521, 650
Bath, G. T., & Pringle, J. E. 1981, MNRAS, 194, 967
Buat-Ménard, V., & Hameury, J.-M. 2002, A&A, 386, 891
Buat-Ménard, V., Hameury, J.-M., & Lasota, J.-P. 2001, A&A, 366, 612
Cannizzo, J. K. 1993a, in Accretion Disks in Compact Stellar Systems, ed. J. C. Wheeler (Singapore: World Scientific), 6 (C93a)
Cannizzo, J. K. 1993b, ApJ, 419, 318 (C93b)
Cannizzo, J. K. 1994, ApJ, 435, 389
Cannizzo, J. K. 1998a, ApJ, 493, 426
Cannizzo, J. K. 1998b, ApJ, 494, 366
Cannizzo, J. K. 2001a, ApJ, 556, 847
Cannizzo, J. K. 2001b, ApJ, 561, L175
Cannizzo, J. K., Gehrels, N., & Mattei, J. A. 2002, ApJ, 579, 760
Cannizzo, J. K., & Mattei, J. A. 1992, ApJ, 401, 642
Cannizzo, J. K., & Mattei, J. A. 1998, ApJ, 505, 344
Cannizzo, J. K., & Wheeler, J. C., 1984, ApJS, 55, 367
Cannizzo, J. K., Wheeler, J. C., & Polidan, R. S. 1986, ApJ, 301, 634 (C86)
Faulkner, J., Lin, D. N. C., & Papaloizou, J. 1983, MNRAS, 205, 359
Frank, J., King, A. R., & Raine, D. J. 2002, Accretion Power in Astrophysics, 3rd ed. (Cambridge: Cambridge Univ. Press)
Gammie, C. F. 1996, ApJ, 457, 355
Gammie, C. F., & Menou, K. 1998, ApJ, 492, L75
Hameury, J.-M., Menou, K., Dubus, G., Lasota, J.-P., & Hure, J.-M. 1998, MNRAS, 298, 1048 (H98)
Hirose, S., Krolik, J. H., & Blaes, O. 2009, ApJ, 691, 16
Hoffmeister, C., 1966, Astron. Nachr., 289, 139
Howell, S. B., Ciardi, D. R., Szkody, P., van Paradijs, J., Kuulkers, E., Cash, J., Sirk, M., & Long, K. S. 1999, PASP, 111, 342
Howell, S. B., Nelson, L. A., & Rappaport, S. 2001, ApJ, 550, 897
Ichikawa, S., Hirose, M., & Osaki, Y. 1993, PASJ, 45, 243
Ichikawa, S., & Osaki, Y. 1992, PASJ, 44, 15
Ichikawa, S., & Osaki, Y. 1994, PASJ, 46, 621
Kato, T. 1993, PASJ, 45, L67
Kato, T., Poyner, G., & Kinnunen, T. 2002, MNRAS, 330, 53
King, A. R., & Pringle, J. E. 2009, MNRAS, 397, L51
King, A. R., Pringle, J. E., & Livio, M. 2007, MNRAS, 376, 1740
Kolb, U., King, A. R., & Ritter, H. 1998, MNRAS, 298, L29
Lasota, J.-P. 2001, New Astron. Rev., 45, 449
Lightman, A. P. 1974, ApJ, 194, 419
Lin, D. N. C., Papaloizou, J., & Faulkner, J. 1985, MNRAS, 212, 105
Lubow, S. H. 1991a, ApJ, 381, 259
Lubow, S. H. 1991b, ApJ, 381, 268
Lubow, S. H., & Shu, F. H. 1975, ApJ, 198, 383
Ludwig, K., & Meyer, F. 1998, A&A, 329, 559
Menou, K. 2000, Science, 288, 2022
Menou, K., Hameury, J.-M., & Stehle, R. 1999, MNRAS, 305, 79
Meyer, F. & Meyer-Hofmeister, E. 1981, A&A, 104, L10
Meyer, F. & Meyer-Hofmeister, E. 1982, A&A, 106, 34
Meyer, F. & Meyer-Hofmeister, E. 1984, A&A, 132, 143
Meyer, F. & Meyer-Hofmeister, E. 1994, A&A, 288, 175
Mineshige, S. 1986, PASJ, 38, 831 (M86)
Mineshige, S. 1987, Ap & Sp. Sci., 130, 331 (M87)
Mineshige, S. & Osaki, Y. 1983, PASJ, 35, 377 (M83)
Mineshige, S. & Osaki, Y. 1985, PASJ, 37, 1 (M85)
Mukai, K., Zietsman, E., & Still, M. 2009, ApJ, 707, 652
Osaki, Y. 1989a, in Theory of Accretion Disks, ed. F. Meyer et al. (Kluwer: Dordrecht), 183
Osaki, Y. 1989b, PASJ, 41, 1005
Osaki, Y., & Meyer, F. 2003, A&A, 401, 325
Papaloizou, J., & Pringle, J. E. 1977, MNRAS, 181, 441
Pringle, J. E. 1981, ARAA, 19, 137
Pringle, J. E., Verbunt, F., & Wade, R. A. 1986, MNRAS, 221, 169 (P86)
Schreiber, M. R., Hameury, J.-M., & Lasota, J.-P. 2004, A&A, 427, 621 (S04)
Shakura, N. I., & Sunyaev, R. A. 1973, A&A, 24, 337
Simpson, J. C., & Wood, M. A. 1998, ApJ, 506, 360
Smak, J. 1984, Acta Astr., 34, 161 (S84)
Smak, J. 2004, Acta Astr., 54, 221
Still, M. R., Howell, S. B., Wood, M. A., Cannizzo, J. K., & Smale, A. P. 2010, ApJL, submitted
Whitehurst, R. 1988, MNRAS, 232, 35